



NBSIR 85-3287

# An Experimental/Computational Investigation of Organized Motions in Axisymmetric Coflowing Streams

---

R. W. Davis

U.S. DEPARTMENT OF COMMERCE  
National Bureau of Standards  
Center for Chemical Engineering  
Gaithersburg, MD 20899

December 1985

Prepared for:

Force Office of Scientific Research/NA  
ing Air Force Base  
nington, DC 20332

QC  
100  
.U56  
85-3287  
1985



NBSIR 85-3287

NBS  
RESEARCH INFORMATION  
CENTER

**AN EXPERIMENTAL/COMPUTATIONAL  
INVESTIGATION OF ORGANIZED  
MOTIONS IN AXISYMMETRIC  
COFLOWING STREAMS**

---

Ref. NBS  
QC100  
U56  
no. 85-3287  
1985

R. W. Davis

U.S. DEPARTMENT OF COMMERCE  
National Bureau of Standards  
Center for Chemical Engineering  
Gaithersburg, MD 20899

December 1985

Prepared for:  
Air Force Office of Scientific Research/NA  
Bolling Air Force Base  
Washington, DC



---

U.S. DEPARTMENT OF COMMERCE, Malcolm Baldrige, *Secretary*  
NATIONAL BUREAU OF STANDARDS, Ernest Ambler, *Director*



TABLE OF CONTENTS

Abstract . . . . .	1
Introduction . . . . .	2
Experimental Results . . . . .	4
Computational Results . . . . .	9
Concluding Remarks . . . . .	14
Acknowledgments . . . . .	15
References . . . . .	15



AN EXPERIMENTAL/COMPUTATIONAL INVESTIGATION  
OF ORGANIZED MOTIONS IN AXISYMMETRIC COFLOWING STREAMS

R. W. Davis  
Center for Chemical Engineering  
National Bureau of Standards  
Gaithersburg, MD 20899

A joint experimental/computational investigation of the entrainment process in the turbulent mixing of a round jet with a coflowing stream has been carried out. The overall objectives of this work were to identify and characterize coherent motions in the mixing region, investigate the dynamical role these motions play in the entrainment process, and determine the extent to which entrainment is affected by such factors as initial conditions and forcing.

It has been found experimentally that, in contrast to the free jet and to previous theoretical predictions based on convected free jet velocity profiles, the coflowing jet undergoes a streamwise evolution in scaling characteristics. The wake region near the origin of the jet is responsible for a streamwise variation in spectra and for a streamwise acceleration of excited waves. Both effects can be scaled by using the average of the jet core velocity and the local minimum mean velocity. The proper scaling parameter downstream of the wake region is found to be the same as for a plane mixing layer, namely,  $(U_j - U_e)/(U_j + U_e)$ . Linear parallel flow stability theory has been found to agree qualitatively with the measurements, but does not produce accurate quantitative predictions of spatial growth rates.

The computational portion of this investigation has produced numerical models for forced spatially-developing axisymmetric and two-dimensional

mixing layers. The numerical scheme employs quadratic upwind differencing for convection and a Leith type of temporal differencing in order to solve the incompressible Navier-Stokes and continuity equations. The applied forcing function is derived from linear inviscid stability theory. The resulting large-scale vortex dynamics is visualized by means of streakline and isovorticity contour plots. It is seen that the vortex merging behavior in both types of mixing layers is determined by the subharmonics present in the forcing function. Manipulation of the vortex dynamics in a predictable fashion is possible through alterations in the frequency content of this applied forcing. Reynolds number is shown to be of only minor importance. Computations of differentially-heated two-dimensional mixing layers have produced some quantitative measures of downstream entrainment and its relationship to the large-scale structures.

Key Words: Coherent structures; computational methods; fluid dynamics; hydrodynamic instability; jets; mixing layers; turbulence

## Introduction

Rapid mixing in coflowing streams is essential to high performance in thrust augmenting ejectors and in air breathing combustors where mixing must be accomplished within the short lengths available in aircraft applications. Advances in these technologies have been limited to a large extent by an incomplete understanding of the dynamics of turbulent mixing. While complex geometries are encountered in applications, the rational development of these technologies requires a more complete understanding of the fundamental fluid dynamics in carefully controlled experimental situations involving simple geometries, such as that discussed herein, where the effects of basic parameters can be isolated and identified.

Stimulated both by the classical Reynolds decomposition of the Navier-Stokes equations and by the experimental ease of acquiring time-averaged information from fixed probes, traditional approaches to the study of turbulent mixing have been primarily statistical in nature, regarding turbulence as an essentially random process involving a continuous distribution of "eddy" scales. This view has been modified substantially over the last decade and a half, giving way to a mounting body of experimental evidence for the existence of highly organized coherent motions in turbulent flows. The limitations and inadequacies of the traditional approaches have been well documented in a number of recent and excellent review papers [1-4], and these arguments will not be repeated here. The important point is that both flow visualization and minicomputer-based conditional sampling techniques are leading to a new view of turbulent motions wherein organized structures play a dominant and deterministic role in turbulent processes. This, coupled with recent advances in computational fluid dynamics, has opened the door to a new level of understanding, and it is this combined approach which has been employed in the present investigation. This investigation has consisted of a joint experimental-computational study of the entrainment process in the turbulent mixing of a round jet with a coflowing stream. The overall objectives of this work were to identify and characterize coherent motions in the mixing region, investigate the dynamical role these motions play in the entrainment process, and determine the extent to which entrainment is affected by such factors as initial conditions and forcing.

The results of the present investigation have already been discussed in detail in a series of technical papers and reports [5-10]. Thus only a summary of what has been accomplished will be presented here.

## Experimental Results

Particular experimental objectives included evaluating the applicability of linear parallel stability theory to the early shear layer, examining the influence of the inner and outer boundary layers of the jet apparatus (and the resulting wake region in the early velocity profiles), and determining the proper relationships between the free and the coflowing jet characteristics.

The experiments were performed on an air jet apparatus (Fig. 1) mounted on the test section centerline of the Low Velocity Wind Tunnel at the National Bureau of Standards [11]. The wind tunnel provided the external (coflowing) air stream with a turbulence level of 0.05% outside the boundary layer of the jet apparatus. The inside diameter of the jet tube was 44.4 mm (1.75 inches) and the wind tunnel test section 0.91 m by 0.91 m (3 ft by 3 ft) so that the area ratio was 535:1. Screens and a flow straightener inside the jet pipe and near the exit produced a jet velocity profile having a nearly constant velocity core and a nearly uniform core turbulence intensity of 0.9 to 1.1%. The wind tunnel and the jet were both generally operated over the speed range of 1 to 6 m/s. The velocity data were acquired by a minicomputer system [12] from a single hot-wire probe (Pt, 2.5  $\mu\text{m}$  by 0.5 mm) and a constant temperature hot-wire anemometer.

It is now widely recognized that acoustic characteristics of a jet apparatus are of great importance in determining the development of the shear layer, at least for laminar and quasi-laminar flows [13]. For the present work the acoustic effects were particularly strong since the apparatus consisted of a straight pipe of constant diameter only 2.4 m in length, an effective resonator. To determine the acoustic characteristics, a microphone was inserted near the closed end of the pipe and low level

acoustic waves were excited by a rotating perforated disc located in the air supply line. The results (Fig. 2) show a set of resonances having a spacing in frequency corresponding approximately to that predicted by a simple acoustic analysis.

The stability calculations used here were based on the analysis of Michalke and Hermann [14] for an incompressible, inviscid, axisymmetric coflowing jet. The computational procedure used was developed independently, however, and is reported by Moore [10]. Locally parallel flow and small amplitude spatially developing disturbances are assumed so that the Euler equations may be linearized and satisfied by a disturbance of the form

$$\phi' = \phi(r)e^{i(\alpha x - \beta t)}$$

where  $\phi$  may be  $u$ ,  $v$ , or  $p$ ;  $\alpha$  is the complex wave number,  $\beta$  the real frequency,  $r$  the radial coordinate,  $x$  the streamwise coordinate, and  $t$  the time. These have been nondimensionalized using the jet core velocity,  $U_j$ , and the inside radius of the jet pipe,  $R$ . The resulting equations were then solved numerically using curves fit to measured mean velocity profiles by a least squares procedure. Note that these profiles were not derived in any way from free jet data, but are measured profiles for the coflowing jet. Thus they include the remnants of the jet-pipe boundary layers which form a decaying wake-like region.

Neither nonparallel flow nor finite disturbance amplitudes is accounted for by this analysis. Yet it is quite likely that some of the differences observed between the analytical results and the measurements are due to

these features. There has been some work on extending the basic theory to slowly diverging flows and to weakly nonlinear flows (see ref. 15 for a review). Here, however, these aspects have not been pursued.

The mean velocity profiles are complicated functions of radius,  $r$ , downstream distance,  $x$ , the core exit velocity of the jet,  $U_j$ , and the velocity of the external stream far from the jet,  $U_e$ . Five combinations of  $U_j$  and  $U_e$  were investigated in detail for which selected profiles are plotted in Figs. 3-5. The most apparent characteristic of these profiles is the decaying wake region resulting from the boundary layers on the jet pipe walls. For purposes of discussion this wake region may be described in terms of an inner and an outer shear layer with a gradual disappearance of the outer shear layer. The inner shear layer here is much steeper than the outer thus having in some ways a much stronger influence on the stability characteristics. However, these results should be viewed with some caution since very different characteristics might develop if the outer layer were steeper than the inner layer. This possibility has not been explored here, but perhaps warrants further investigation.

It has been found that the effects of a coflowing stream on a round jet cannot be determined by simply transforming a free jet flowfield to a coordinate system moving at the coflowing stream velocity, at least not for facilities in which the flow develops rapidly near the jet origin. The only exception, it would seem, would be a facility in which acoustic resonances have been eliminated (in the unstable range of frequencies) and in which the background disturbances have been reduced to unusually low levels. In such a flow the streamwise development of waves might extend far beyond the region where the wake of the jet pipe is important. In most coflowing jets,

however, this will not be the case and the wake region must be taken into account. In that region it has been found that the flow evolves, not simply in magnitude but in fundamental scaling characteristics. The rapidly changing velocity profiles cause large variations in the spatial growth rates of waves leading to streamwise variations in spectra and in wave speed. The influence of the external stream speed,  $U_e$ , is not simple, however. Near the jet origin the spectra and wave speeds are nearly independent of  $U_e$ , whereas further downstream the influence is substantial. Any scaling laws for this flow must be able to account for the observed evolution. In particular, the usual choices for characteristic velocity, for instance  $U_j + U_e$ , must be modified. An alternative proposed here,  $U_j + U_m$ , where  $U_m$  is the minimum mean speed in a cross-stream profile, is found to satisfactorily scale both spectra and wave speeds. It is furthermore consistent with the concept that the "inner" shear layer in this coflowing jet is dominant because it is substantially stronger than the "outer" shear layer. Since  $U_j + U_m$  approaches  $U_j + U_e$  downstream, the latter would seem to be the proper characteristic velocity beyond the wake region in the flow.

A simple linear, parallel flow stability theory has not fared badly in analyzing this flow. In fact, the work of Michalke and Hermann [14] predicted several of the important characteristics observed in the experiments, including the shift of spectra to higher frequencies as  $U_e$  is increased for positions not near the jet origin and the streamwise acceleration of waves. This was despite the use of transformed free jet profiles. Other predicted results were not borne out, however. A stretching factor,  $\sigma'$ , defined as

$$\sigma' = 1 + \frac{AU_e}{U_j - U_e}$$

was calculated by Michalke and Hermann [14] who inferred a value  $A = 1.4$  for the transformed free jet data. In the present work, however,  $A = 2.0$  is found to provide the best correlation of the coflowing jet measurements. This is in agreement with experiments on the plane mixing layer. For  $A = 2.0$ ,  $\sigma'(U_j - U_e)$  becomes simply  $U_j + U_e$ , the characteristic velocity downstream of the wake region.

Calculations based on the work of Michalke and Hermann [14], but performed on the measured coflowing jet profiles of the present work, likewise agreed with several of the trends in the experimental data. In particular, the cross-stream profiles of wave amplitude compare relatively well with the measurements as did the wave speeds near the jet origin. The predictions of streamwise growth were more difficult to compare with the NBS measurements due to the rapid development of the profiles and corresponding changes in the calculations. However, the bracketing of the data by the calculations would seem to indicate at least qualitative agreement. As a whole the linear, parallel flow, stability theory did not fare badly, but could possibly be improved by taking into account the nonparallel and weakly nonlinear aspects of the flow.

Finally, it should again be noted that the complexity of the coflowing jet configuration and the dependence of the flow properties on so many factors should be taken into account in any attempts to apply the results presented here to other facilities. The relative importance of the two initial boundary layers in particular should be viewed with caution. An

interesting, though perhaps difficult, experiment would be to repeat the measurements performed here but for an apparatus in which the outer boundary layer is much thinner and steeper than the inner one. This might have profound effects on the flow characteristics.

### Computational Results

The primary computational objective of this investigation was to develop a numerical model for the large-scale vortex dynamics inside forced spatially-developing axisymmetric mixing layers. The temporally-developing case, with its simpler boundary conditions, had been modeled previously [15], but was not a completely plausible representation of what occurs inside the mixing layer between a jet and a coflowing stream. The axisymmetry condition implies that azimuthal instabilities were not considered here. This is a realistic assumption (at least in the near-field) provided that axisymmetric forcing is employed.

The axisymmetric mixing layer develops in the region between a jet with velocity  $U_j$  and a coflowing stream with velocity  $U_\infty$ . Therefore, at the upstream boundary of the computational domain ( $z = 0$ ), a velocity profile  $U(r)$  characteristic of a coflowing jet is specified. This profile contains a shear layer centered at  $r = R_j$  which develops into the mixing layer for  $z > 0$ . In an unforced physical experiment, random background noise will supply the perturbation necessary to trigger roll-up of this shear layer. The particular component of the background noise which is responsible for the initial vortex formation can be determined from linear inviscid stability theory as that frequency which exhibits the largest spatial growth rate [14]. Thus, for the computations, a perturbation of the form

$$\sum_n A_n(r) \exp \{i[R(\alpha_n)z - \beta_n t]\}$$

is applied to the vorticity over some streamwise region from  $z = 0$  to  $z = z_p \geq 0$ . Here  $A_n(r)$  are complex eigenfunctions,  $R(\alpha_n)$  is the real part of a complex  $\alpha_n$ , and  $\beta_n$  is real. When it is desired to match the situation in an unforced physical experiment, all parameters are chosen so as to minimize  $\text{Im}(\alpha_1)$  [14, 16]. In the case of a forced physical experiment, the  $\beta_n$  for  $n > 1$  must be subharmonics of  $\beta_1$ , i.e.,  $\beta_1$  is an integer multiple of  $\beta_2$ , another integer multiple of  $\beta_3$ , etc. [16]. Variations in the amplitude and domain of the applied perturbation have been found not to affect the resulting vortex dynamics in any fundamental way. For this study, the maximum amplitude of the perturbation was about  $0.01 U(r)$  and  $z_p = 2R_j$ . Reynolds number ( $Re$ ) based on  $U_j$  and  $R_j$  has also been found not to affect the basic vortex dynamics although the vortices do smear out as  $Re$  decreases.

A finite difference method was employed here in order to solve the incompressible Navier-Stokes and continuity equations in primitive variables on a staggered mesh. This method utilized quadratic upwind differencing for convection and an explicit Leith-type of temporal differencing [7]. This leads to effectively third-order accurate spatial differencing as  $Re \rightarrow \infty$ . The only relevant stability criterion is that the Courant number be less than one. This type of differencing scheme has been shown to perform well in computing vortex shedding from bluff bodies [17, 18]. At each time step a Poisson equation for pressure was solved by a direct method utilizing the

FISHPAK package of FORTRAN subprograms for the solution of separable elliptic partial differential equations developed at NCAR [19]. No turbulence model was employed in this computation.

The boundary conditions in the radial direction employed here were that radial derivatives are set to zero along  $r = 0$  (axisymmetry), and a simple asymptotic analysis involving small perturbations about  $U_\infty$  was employed for large  $r$ . The freestream velocity  $U_\infty$  was specified at the outflow boundary of the mesh by means of an infinite-to-finite mapping of the form  $\zeta = K + K_1/z$ , where  $K$  and  $K_1$  are constants. This transform was employed for  $z > 15 R_j$ .

The untransformed portion of the nonuniform mesh used here is shown in Fig. 6, where it can be seen that mesh points are concentrated in the region of the initial shear layer near  $r = 1$ . The length scales in Fig. 6 are normalized with respect to  $R_j$ . All results that follow are nondimensionalized with respect to  $R_j$  and  $U_j$ . Computation times on the NBS UNIVAC 1100/82 required to obtain a few unchanging cycles of vortex dynamics were typically about 3 hours.

A plot of an upstream velocity profile with  $U_j/U_\infty = 3.33$  is shown in Fig. 7. This profile, consisting of two Gaussians matched (with continuous first derivatives) at  $r = 1$ , is typical of what is found downstream of a jet nozzle. A linear inviscid stability analysis reveals the most unstable frequency to be  $\beta_1 = 3.48$ . The results of perturbing this velocity profile with  $\beta = \sum_n \beta_n = \beta_1$  (no subharmonics) are shown in Figs. 8 and 9 for  $Re = 1000$ . These two figures illuminate the same flowfield, the first by means

of a streakline plot composed of passive marker particles and the second by means of isovorticity contours. What is seen here is the formation of vortices which shear as they move downstream but do not merge. Figures 10 and 11 show the effects of adding a subharmonic ( $\beta = \beta_1 + \beta_1/2$ ) to the applied perturbation. A single vortex merging is now seen to occur. Adding a second subharmonic ( $\beta = \beta_1 + \beta_1/2 + \beta_1/3$ ) results in two vortex mergings, as shown in Figs. 12 and 13. Thus, each subharmonic induces one merging, as seen experimentally in the two-dimensional mixing layer [16]. By applying only the fundamental and the second subharmonic ( $\beta = \beta_1 + \beta_1/3$ ), three vortices merge into one (Figs. 14 and 15), a phenomenon also seen experimentally [16]. Changing the Reynolds number from 1000 to 333 results in the increased smearing of the vortices (with no change in the merging behavior) seen in Fig. 16 for  $\beta = \beta_1 + \beta_1/2 + \beta_1/3$ . For  $Re = 10^4$  and this same  $\beta$ , the total streamwise energy content integrated across a plane cutting through the jet as a function of axial distance downstream is shown in Fig. 17 for each of the three frequencies. The axial locations where each subharmonic saturates are, in fact, the same as the merging locations as seen from streakline and isovorticity contour plots. Also, the second subharmonic saturates at twice the distance from the upstream profile as the first. All this is, once again, in agreement with experimental results from the two-dimensional mixing layer [16].

In fact, once the axisymmetric mixing layer had been modeled, extension to the two-dimensional case became straightforward. The resulting basic vortex dynamics was observed to be identical to that seen in the axisymmetric situation, i.e., each subharmonic induced one merging. A

phenomenon clearly seen in the two-dimensional case was "vortex shredding" (Fig. 18). This occurred in the presence of a fundamental and its first subharmonic when the subharmonic was phase-shifted by  $\phi = 90^\circ$ . What is clearly seen in Fig. 18 is that the vortex centered at  $x = 110$  is being pulled apart (shredded) by its neighbors. This same sort of phenomenon has been seen before in computations of temporally-developing mixing layers [15]. When compared with the normal vortex merging seen in the zero phase shift case (Fig. 19), it is clear that downstream entrainment is severely reduced by this shredding phenomenon. Full details on both the axisymmetric and two-dimensional mixing layer computations are reported in Davis and Moore [9].

In a further effort to quantify the downstream entrainment process in a two-dimensional mixing layer, differential heating of the two incoming streams was applied. With no gravitational effects in the model, the temperature then acted as a passive contaminant. For the case shown in Fig. 20 (tanh profile at  $x = 0$  with velocity ratio = 3.33, fundamental plus first subharmonic present), the upper high speed stream (for  $y > 0$ ) enters with temperature  $T = 1$ , while the lower stream has  $T = 0$ . The following integrals were then computed:

$$A_I(x) = \int_{-\infty}^0 T \, dy,$$

$$A_O(x) = \int_0^{\infty} (1 - T) \, dy,$$

where in the actual numerical integrations,  $\pm \infty$  were replaced by  $\pm 80$ . When there is no mixing between the streams, both  $A_I$  and  $A_O$  are zero everywhere. Thus, the deviation of these parameters from zero gives a measure of the mixing which is occurring at a given downstream station. By comparing Figs. 21 and 22 ( $A_I$  and  $A_O$ , respectively) with Fig. 20, the effect of the vortex dynamics on the mixing can clearly be seen. Peaks and valleys in both  $A_I$  and  $A_O$  can be directly related to the vertical position of the braid between the vortices seen in Fig. 20. There is also an asymmetry in the mixing, with the peak value of  $A_I$  being about 50% greater than that of  $A_O$ . Thus, more high speed than low speed fluid is entrained and mixed in the coherent structures, an effect also observed experimentally [20]. The summation of  $A_I$  and  $A_O$  shown in Fig. 23 reveals the expected increase in overall mixing with downstream distance, with the peaks here occurring at the locations of the vortices in Fig. 20.

### Concluding Remarks

Several concluding observations can be made pertaining to the results presented in the previous two sections. First, linear parallel stability theory can provide a great deal of useful information regarding the large-scale structure of forced mixing layers. The effectiveness of linear theory in an obviously nonlinear situation has been noted previously [15, 16]. Also, it is clear that modifications such as the addition of nonparallel and weakly nonlinear effects to the theory could enhance its usefulness. A second conclusion that can be drawn here is that the downstream development of the mixing layer (at least in the near-field) can be controlled by

forcing at appropriate frequencies. The presence of subharmonics and their phase relationships is the determining factor in the downstream behavior of the large-scale structures. The vortex dynamics, in turn, is the determining factor in the entrainment characteristics of the mixing layer. Predictive methods (e.g., gradient diffusion models) which ignore the large coherent structures are doomed to failure. Finally, it is clear that fully three-dimensional models will be required to describe the far-field development of both circular and planar mixing layers. Joint computational/experimental research efforts would appear to be highly desirable here. A cooperative effort on joint data analysis techniques alone would undoubtedly prove extremely beneficial.

#### Acknowledgments

J. M. McMichael and L. P. Purtell carried out the experimental portion of this investigation. The contribution of E. F. Moore to the computational effort was invaluable.

#### References

1. Laufer, J., Ann. Rev. Fluid Mech. 7, p. 307 (1975).
2. Roshko, A., AIAA Journal 14, p. 1349 (1976).
3. Liepmann, H. M., American Scientist 67, p. 221 (1979).
4. Davies, P.O.A.L. and Yule, A. J., J. Fluid Mech. 69, p. 513 (1975).
5. McMichael, J. M., Purtell, L. P., Davis, R. W. and Moore, E. F., AIAA Aerospace Sciences Meeting Paper No. 84-0420 (1984).
6. Purtell, L. P., McMichael, J. M., Davis, R. W., and Moore, E. F., AIAA Shear Flow Control Conference Paper No. 85-0574 (1985).

7. Davis, R. W., in Computational Techniques and Applications: CTAC-83 (ed. J. Noye and C. Fletcher), North-Holland, Amsterdam, p. 51 (1984).
8. Davis, R. W. and Moore, E. F., in Ninth International Conference on Numerical Methods in Fluid Dynamics (ed. Soubbaramayer and J. P. Boujot), Springer-Verlag Lect. Notes in Physics 218, p. 180 (1985).
9. Davis, R. W. and Moore, E. F., Phys. Fluids 28, p. 1626 (1985).
10. Moore, E. F., National Bureau of Standards Internal Report 83-2686 (1983).
11. Purtell, L. P. and Klebanoff, P. S., National Bureau of Standards Tech. Note 989 (1979).
12. Purtell, L. P., National Bureau of Standards Tech. Note 1181 (1983).
13. Gutmark, E. and Ho, C.-M., Phys. Fluids 26, p. 2932 (1983).
14. Michalke, A. and Hermann, G., J. Fluid Mech. 114, p. 343 (1982).
15. Ho, C.-M. and Huerre, P., Ann. Rev. Fluid Mech. 16, p. 365 (1984).
16. Ho, C.-M. and Huang, L. S., J. Fluid Mech. 119, p. 443 (1982).
17. Davis, R. W. and Moore, E. F., J. Fluid Mech. 116, p. 475 (1982).
18. Davis, R. W., Moore, E. F. and Purtell, L. P., Phys. Fluids 27, p. 46 (1984).
19. Swarztrauber, P. and Sweet, R., Nat. Center Atmos. Res. Tech. Note IA-109 (1975).
20. Koochesfahani, M. M., Dimotakis, P. E. and Broadwell, J. E., AIAA Journal 23, p. 1191 (1985).

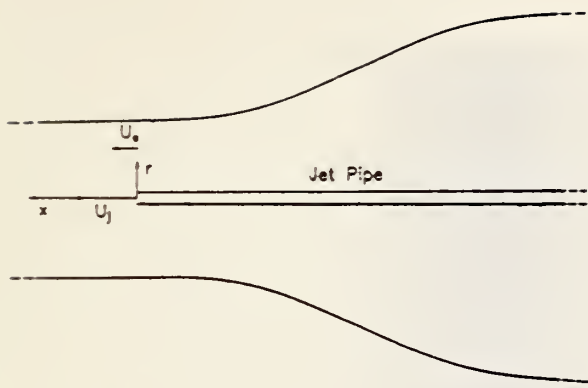


Fig. 1. Schematic of jet apparatus in wind tunnel.

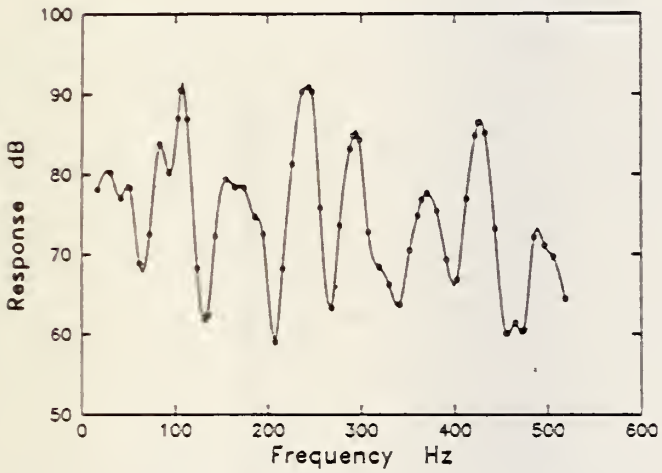


Fig. 2. Acoustic characteristics of jet apparatus.

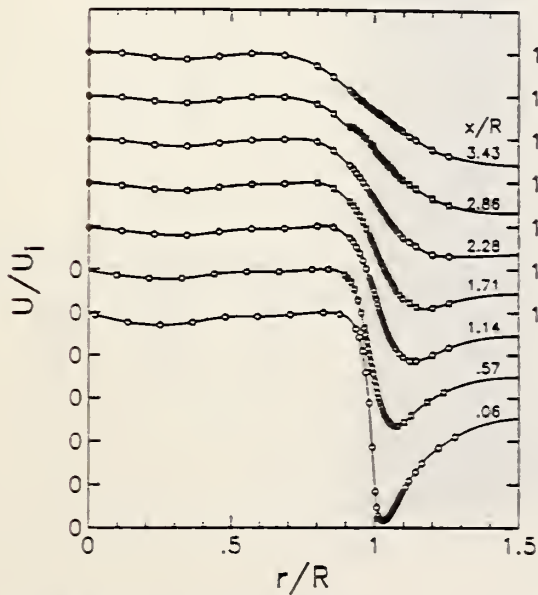


Fig. 3. Mean velocity profiles.  $U_j = 6$ ,  $U_e = 3.0$  m/s.

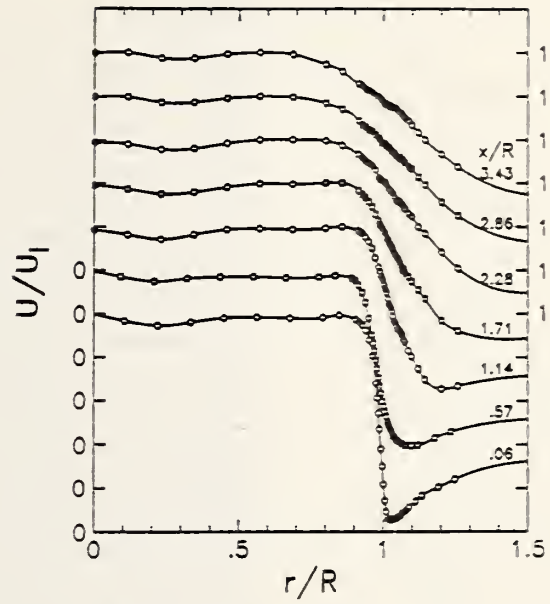


Fig. 4. Mean velocity profiles.  $U_j = 6$ ,  $U_e = 2.0$  m/s.

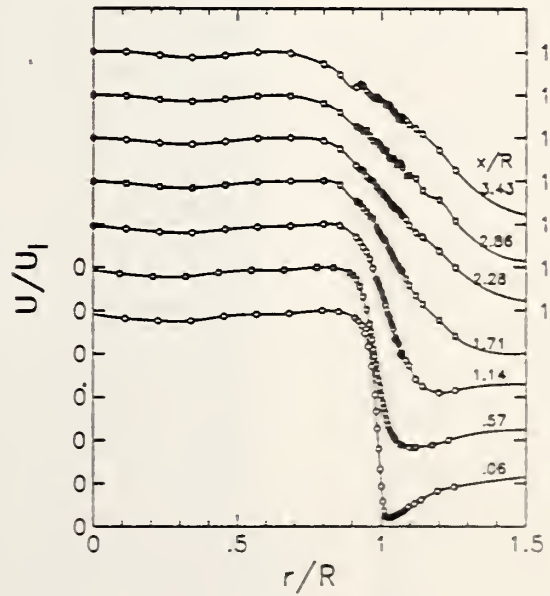


Fig. 5. Mean velocity profiles.  $U_j = 6$ ,  $U_e = 1.5$  m/s.

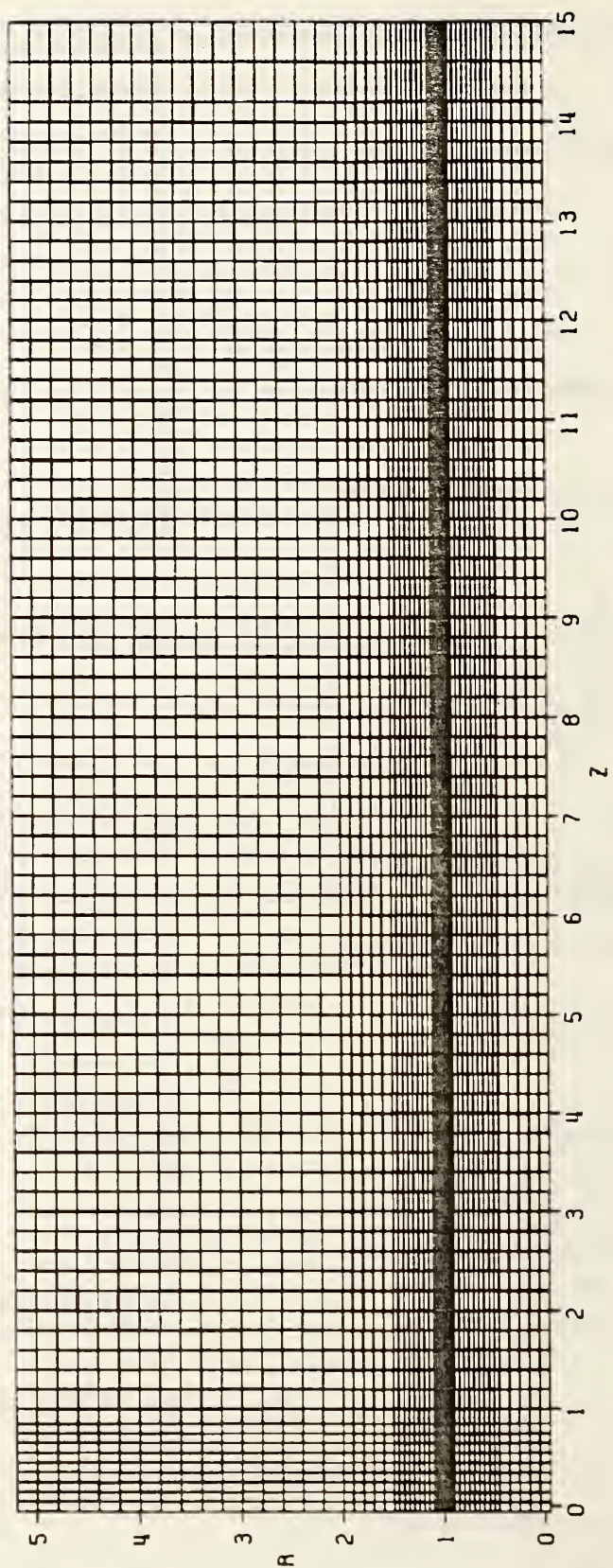


Fig. 6. The 79 x 52 nonuniform mesh.

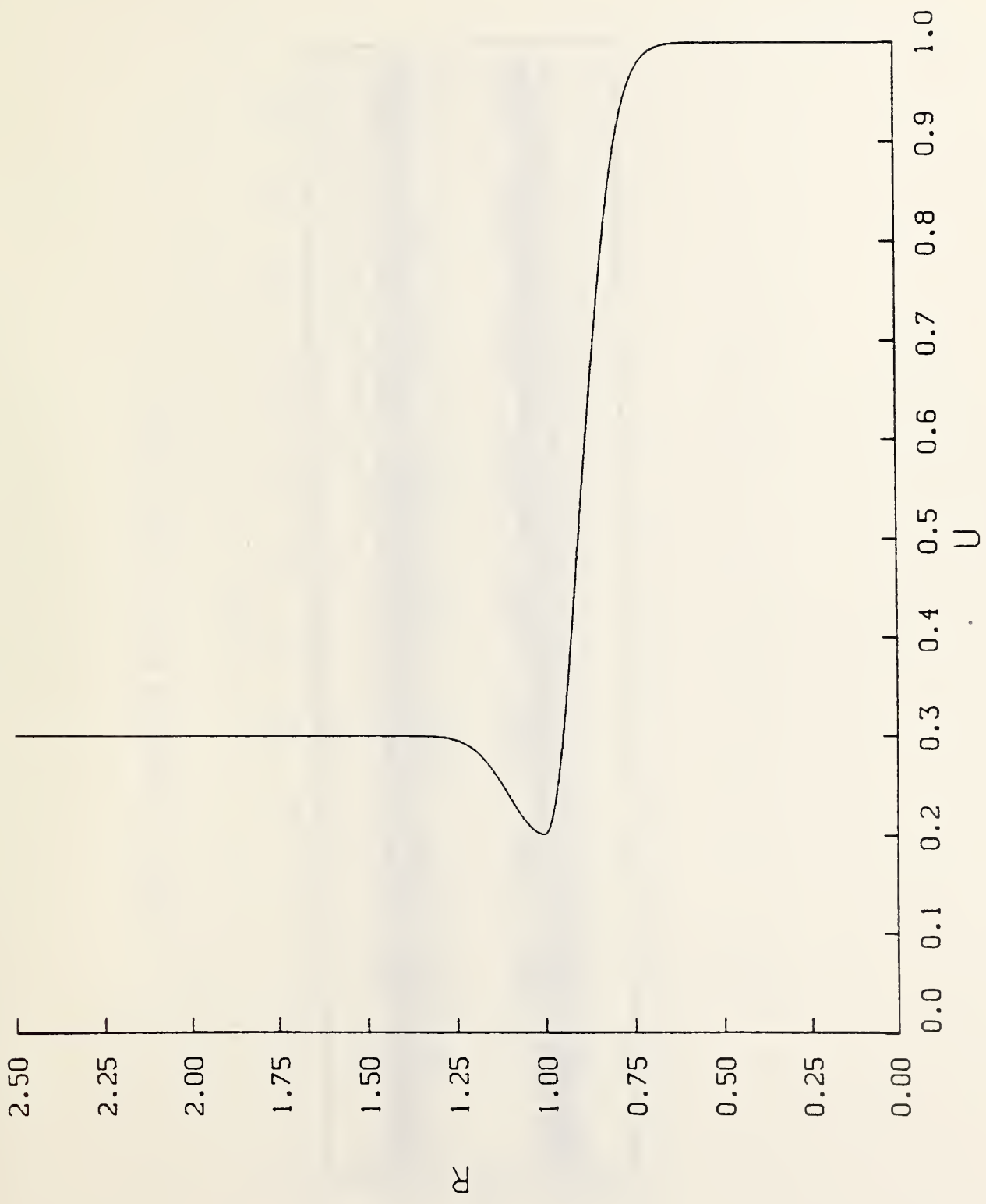


Fig. 7. Upstream velocity profile with  $U_j/U_\infty = 3.33$ .

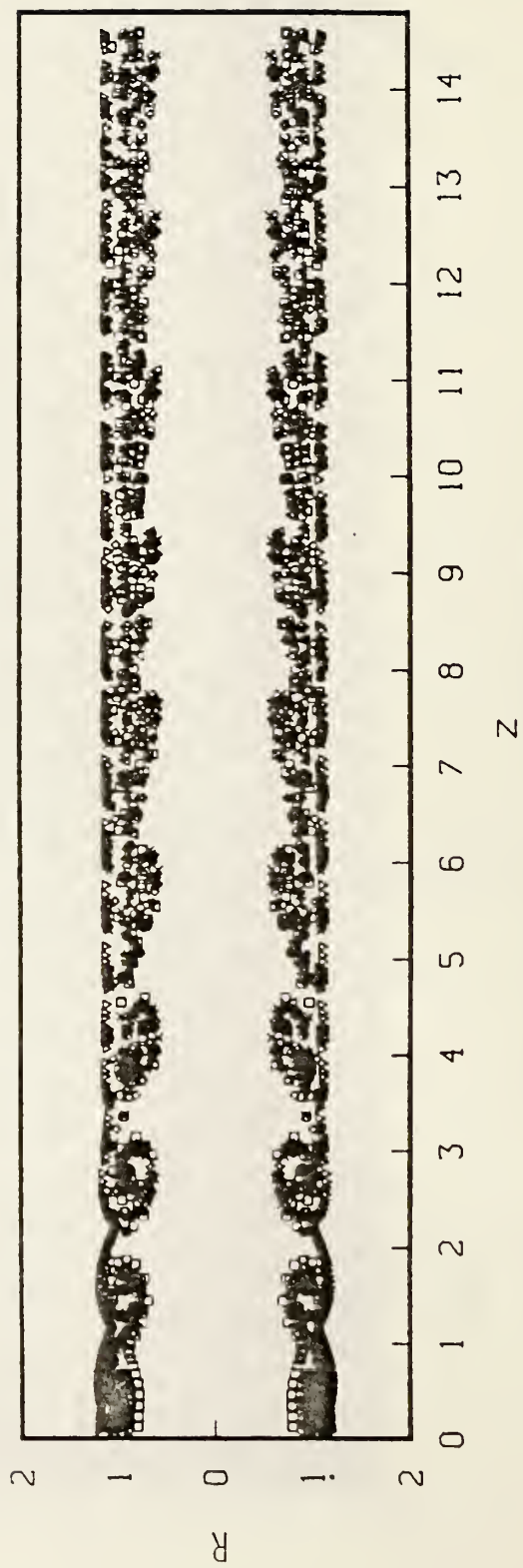


Fig. 8. Streakline plot:  $\beta = \beta_1 = 3.48$ .

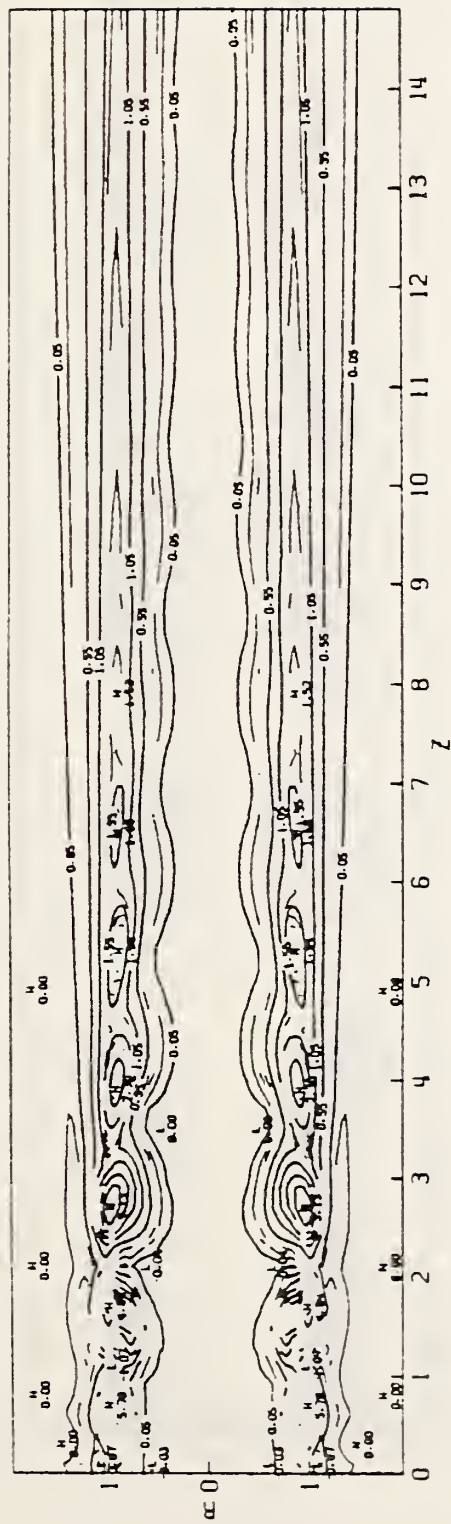


Fig. 9. Isovorticity contour plot:  $\beta = \beta_1 = 3.48$ .

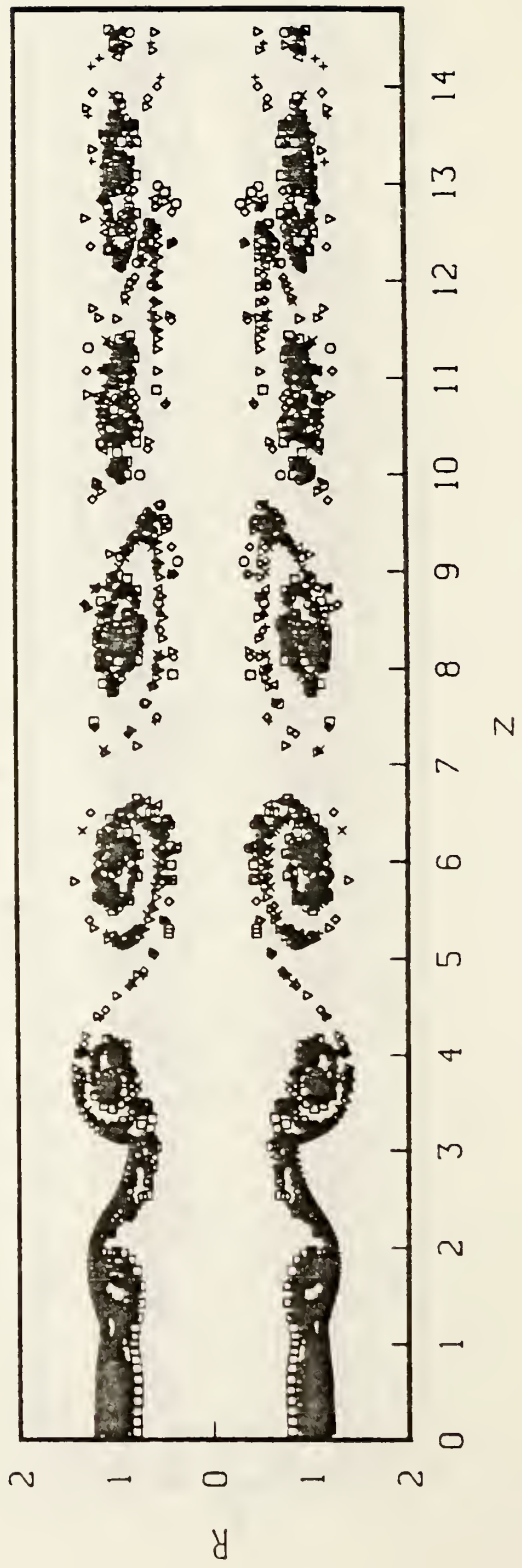


Fig. 10. Streakline plot:  $\beta_1 = 3.48$ ,  $\beta_2 = 1.74$ .

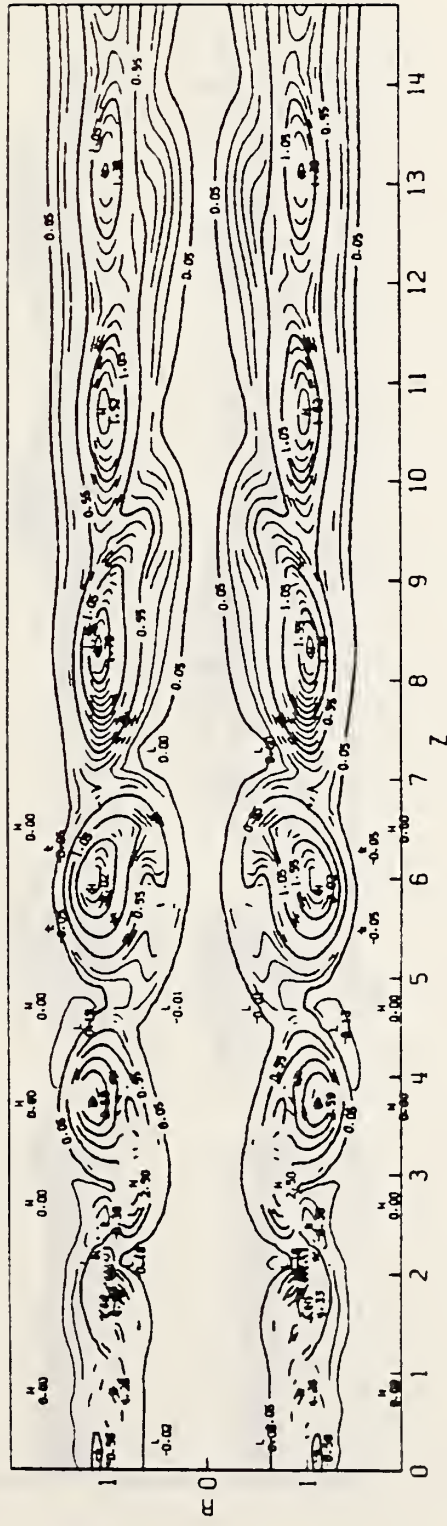


Fig. 11. Isovorticity contour plot:  $\beta_1 = 3.48$ ,  $\beta_2 = 1.74$ .

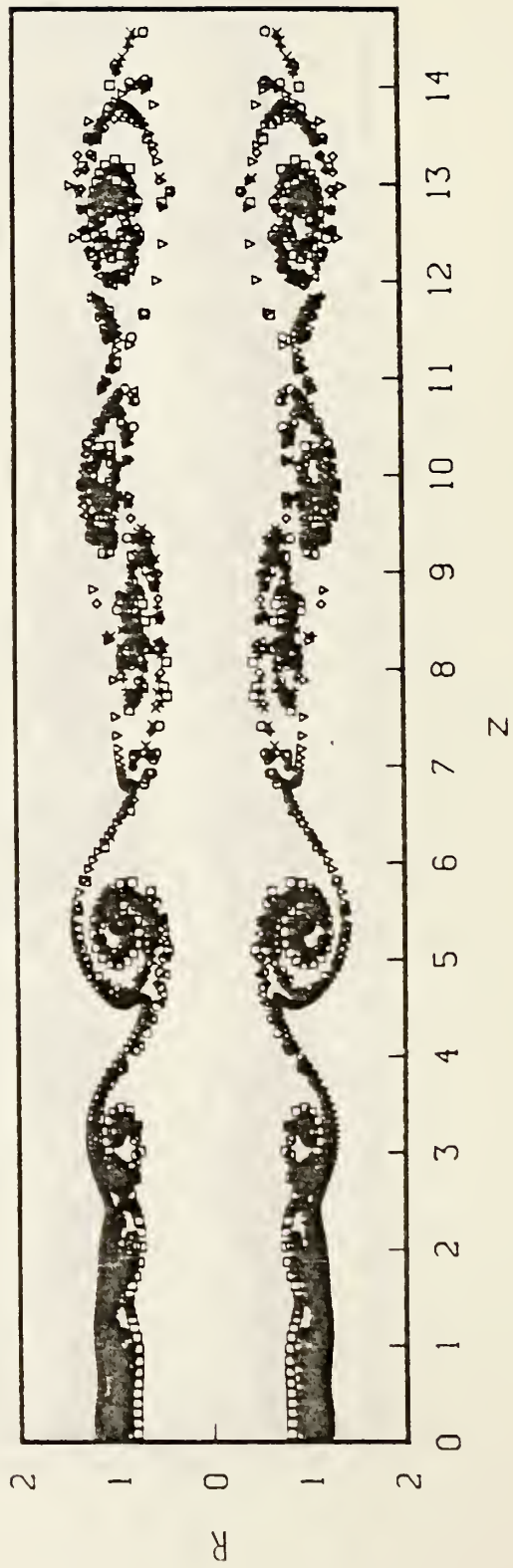


Fig. 12. Streakline plot:  $\beta_1 = 3.48$ ,  $\beta_2 = 1.74$ ,  $\beta_3 = 1.16$ .

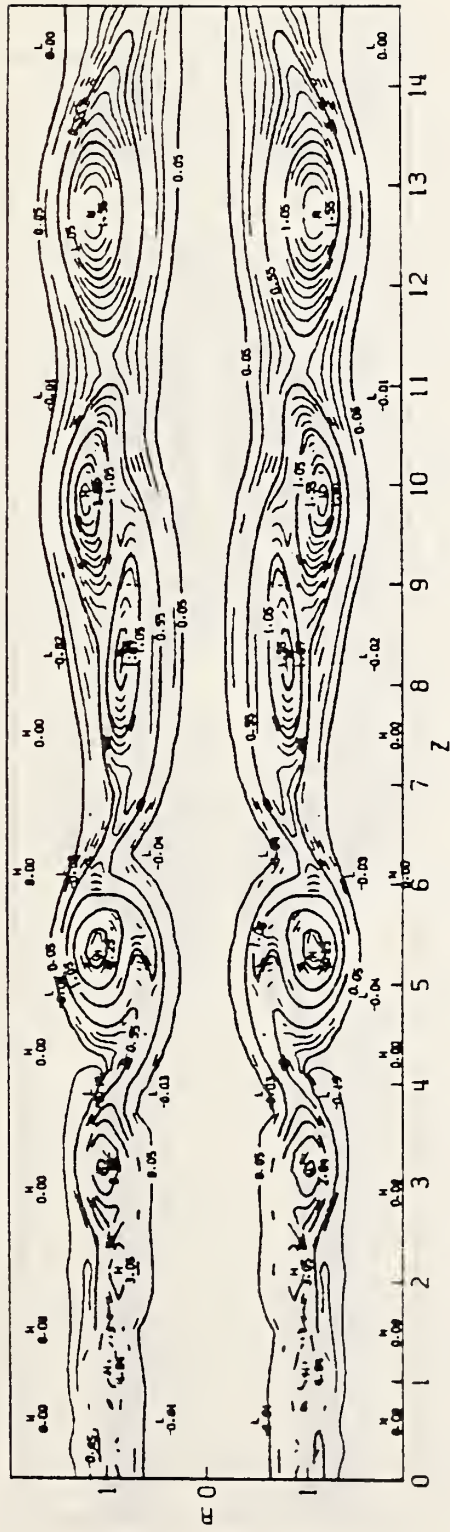


Fig. 13. Isovorticity contour plot:  $\beta_1 = 3.48$ ,  $\beta_2 = 1.74$ ,  $\beta_3 = 1.16$ .

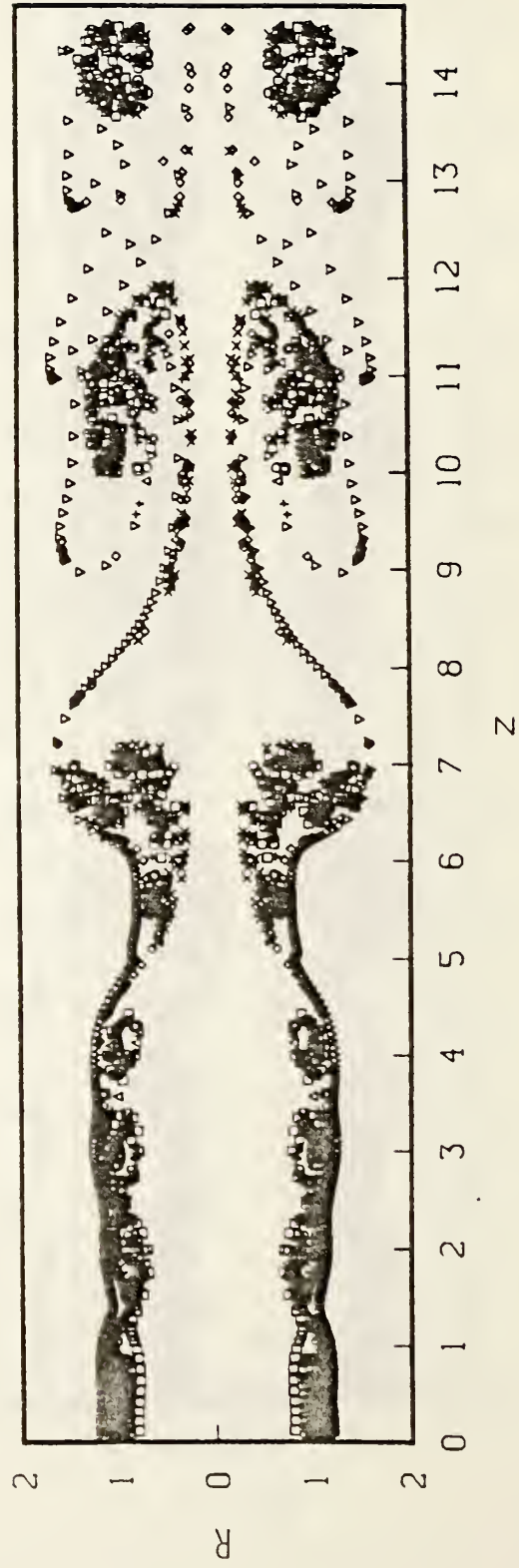


Fig. 14. Streakline plot:  $\beta_1 = 3.48$ ,  $\beta_2 = 1.16$ .





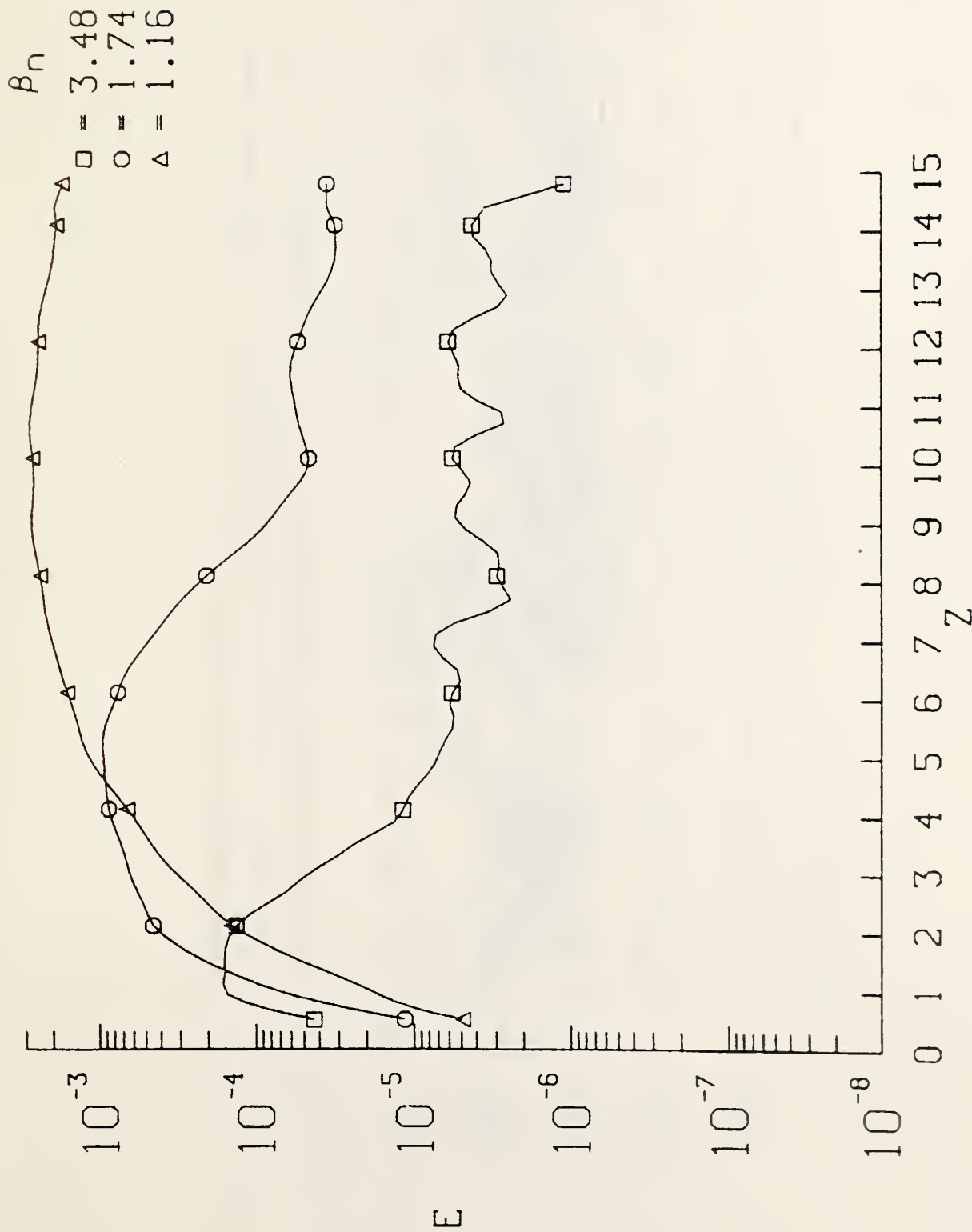


Fig. 17. Streamwise energy content for  $Re = 10^4$ :  $\beta_1 = 3.48$ ,  $\beta_2 = 1.74$ ,  $\beta_3 = 1.16$ .

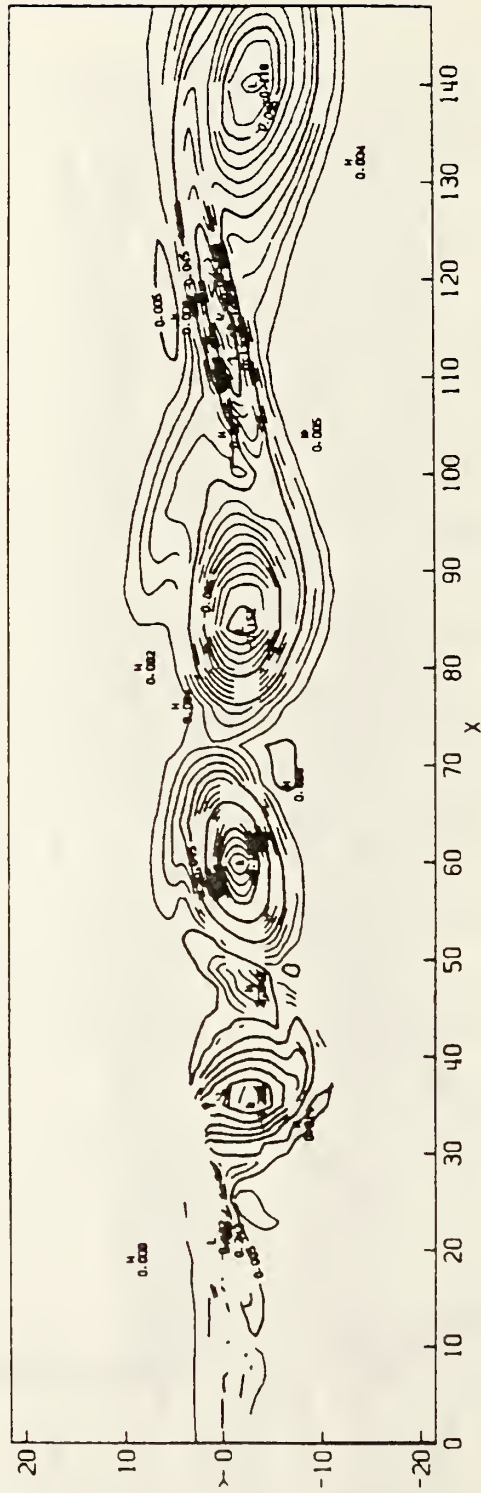


Fig. 18. Isovorticity contour plot of 2-D mixing layer for  $Re = 10^4$ :  $\beta_1 = 0.1425$ ,  $\beta_2 = 0.07125$ ,  $\phi = \pi/2$ . Tanh velocity profile at  $x = 0$  with upper/lower stream velocity ratio = 3.33.

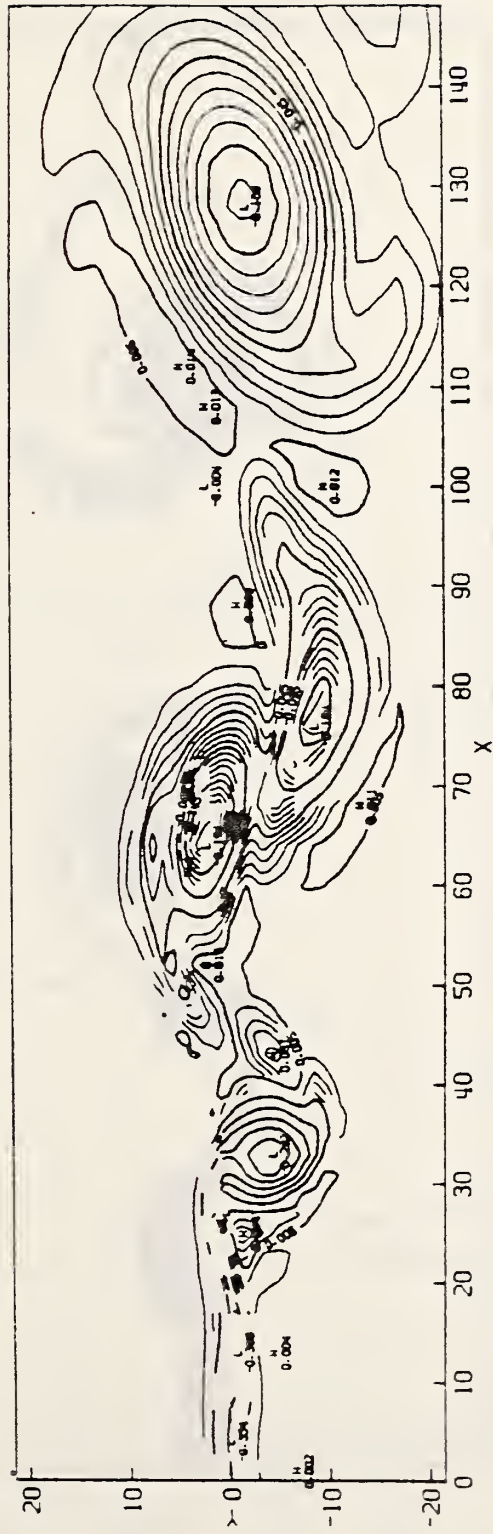


Fig. 19. Isovorticity contour plot of 2-D mixing layer for  $Re = 10^4$ :  $\beta_1 = 0.1425$ ,  $\beta_2 = 0.07125$ ,  $\phi = 0$ . Tanh velocity profile at  $x = 0$  with upper/lower stream velocity ratio = 3.33.

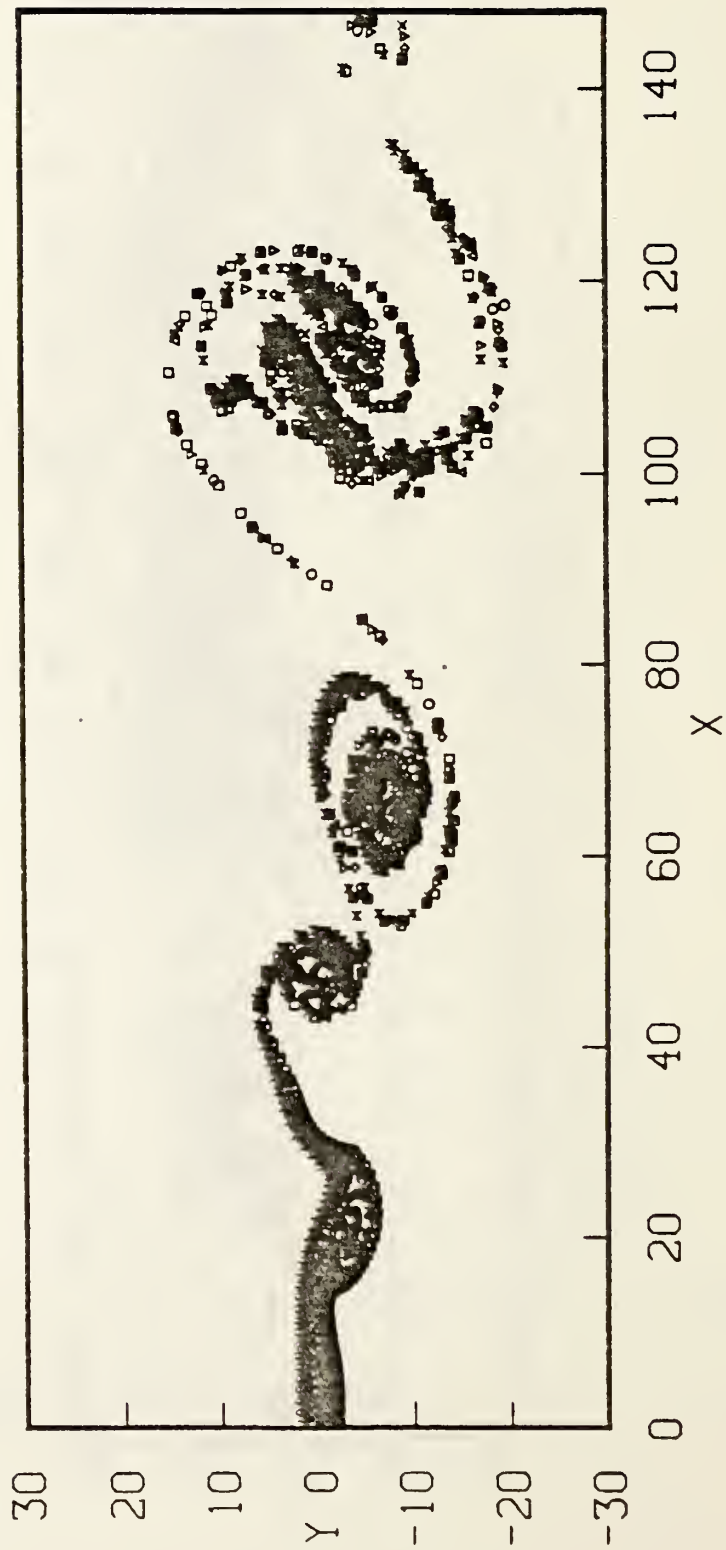


Fig. 20. Streakline plot of 2-D mixing layer for  $Re = 10^4$ :  $\beta_1 = 0.1425$ ,  
 $\beta_2 = 0.07125$

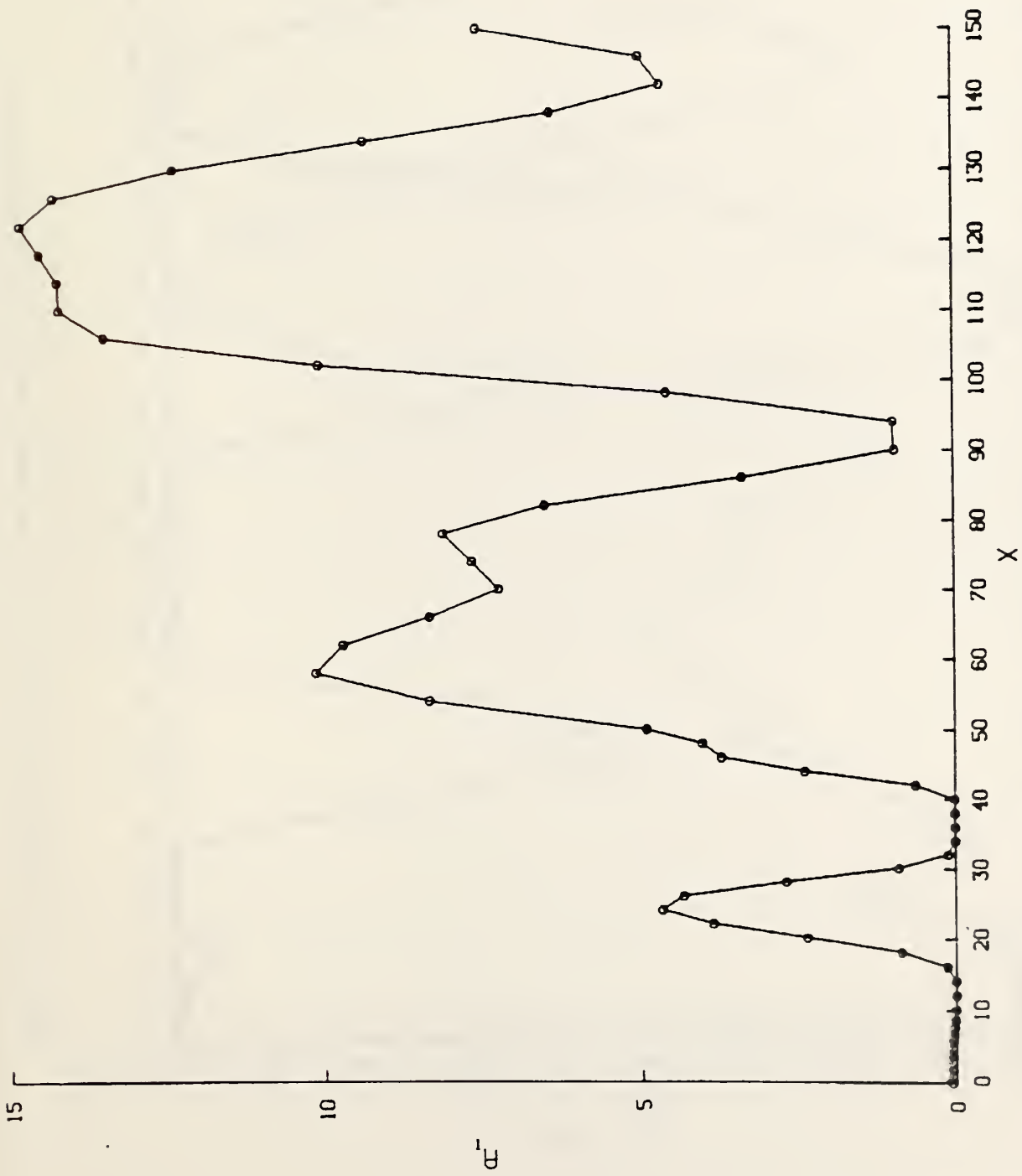


Fig. 21. Downstream variation of  $A_I$  at same instant depicted in Fig. 20.

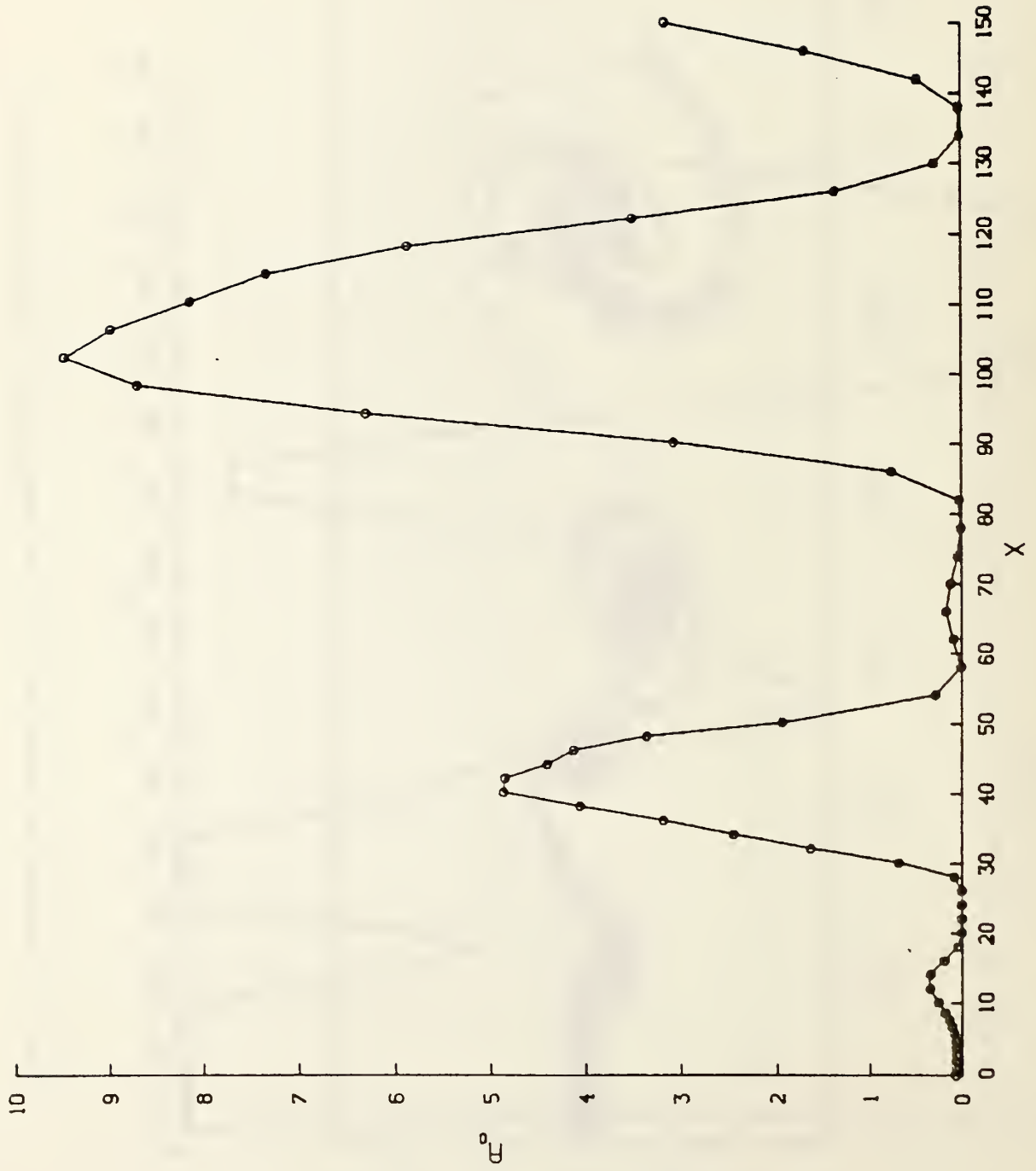


Fig. 22. Downstream variation of  $A_0$  at same instant depicted in Fig. 20.

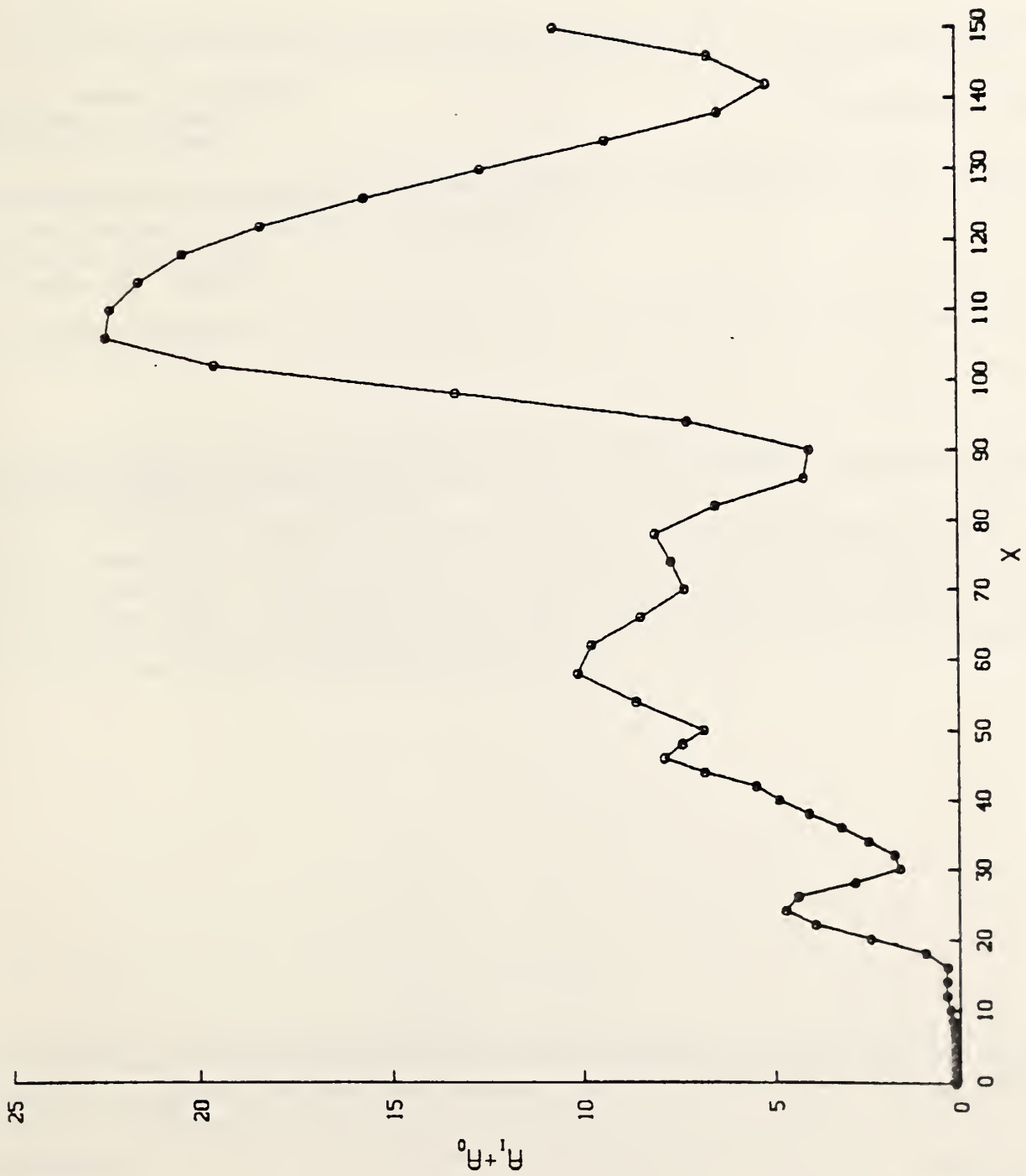


Fig. 23. Downstream variation of  $A_I + A_O$  at same instant depicted in Fig. 20.



U.S. DEPT. OF COMM. <b>BIBLIOGRAPHIC DATA SHEET</b> (See instructions)		1. PUBLICATION OR REPORT NO. NBSIR 85-3287	2. Performing Organ. Report No.	3. Publication Date DECEMBER 1985
4. TITLE AND SUBTITLE An Experimental/Computational Investigation of Organized Motions in Axisymmetric Coflowing Streams				
5. AUTHOR(S) R. W. Davis				
6. PERFORMING ORGANIZATION (If joint or other than NBS, see instructions)  NATIONAL BUREAU OF STANDARDS DEPARTMENT OF COMMERCE WASHINGTON, D.C. 20234			7. Contract/Grant No.	8. Type of Report & Period Covered  Final
9. SPONSORING ORGANIZATION NAME AND COMPLETE ADDRESS (Street, City, State, ZIP) Air Force Office of Scientific Research/NA Dolling Air Force Base Washington, DC 20332				
10. SUPPLEMENTARY NOTES  <input type="checkbox"/> Document describes a computer program; SF-185, FIPS Software Summary, is attached.				
11. ABSTRACT (A 200-word or less factual summary of most significant information. If document includes a significant bibliography or literature survey, mention it here)  A joint experimental/computational investigation of the entrainment process in the turbulent mixing of a round jet with a coflowing stream has been carried out. The overall objectives of this work were to identify and characterize coherent motions in the mixing region, investigate the dynamical role these motions play in the entrainment process, and determine the extent to which entrainment is affected by such factors as initial conditions and forcing.				
12. KEY WORDS (Six to twelve entries; alphabetical order; capitalize only proper names; and separate key words by semicolons) coherent structures; computational methods; fluid dynamics; jets; mixing layers; stability; turbulence				
13. AVAILABILITY  <input checked="" type="checkbox"/> Unlimited <input type="checkbox"/> For Official Distribution. Do Not Release to NTIS <input type="checkbox"/> Order From Superintendent of Documents, U.S. Government Printing Office, Washington, D.C. 20402.  <input checked="" type="checkbox"/> Order From National Technical Information Service (NTIS), Springfield, VA. 22161			14. NO. OF PRINTED PAGES  39	
			15. Price  \$9.95	





